Line Outage Detection Using Phasor Angle Measurements

Joseph Euzebe Tate, *Student Member, IEEE*, and Thomas J. Overbye, *Fellow, IEEE*

***Abstract*—Although phasor measurement units (PMUs) have become increasingly widespread throughout power networks, the buses monitored by PMUs still constitute a very small percentage of the total number of system buses. Our research explores methods to derive useful information from PMU data in spite of this limited coverage. In particular, we have developed an algorithm which uses known system topology information, together with PMU phasor angle measurements, to detect system line outages. In addition to determining the outaged line, the algorithm also provides an estimate of the pre-outage flow on the outaged line. To demonstrate the effectiveness of our approach, the algorithm is demonstrated using simulated and real PMU data from two systems—a 37-bus study case and the TVA control area.**

***Index Terms*-- phasor measurement units, line outages, event detection**

I. Introduction

WITH the increasing loading of the power system, along with the massive inter-area transfers enabled by the deregulation of the 80's and 90's, there is a clear need to have reliable information about both the local system and external systems. Tellingly, four of the six major North American blackouts were due in part to a lack of situational awareness [1]. Although there is a clear need for sharing of information, there is limited real-time sharing of SCADA or state estimator information in the United States [2]. However, as phasor measurement units (PMUs) [3] have been deployed throughout the North American power grid, there have been significant efforts to ensure that PMU data is shared between all interested parties [4]. Because PMU data is more widely available in near real-time than other power system measurement data, it can provide unique insights into the global operation of the grid. However, in order to gain any advantage from this new information, new techniques must be developed to take advantage of the wealth of information that PMUs provide.

Extensive research in applying PMU information to improve situational awareness has been conducted since their introduction, including applications in state estimation [5]-[7], dynamic security assessment [8]-[10], and visualization [11]-[13]. A key aspect of situational awareness in the power grid is the knowledge of transmission line, transformer, and generator statuses. In fact, this information is the major component of the data shared via the NERC System Data Exchange (SDX) [14] . However, the SDX may contain out of date information because updates are only required on an hourly basis [15]. To improve operators' knowledge of grid conditions, particularly in the short term, a method is proposed for quickly detecting line outages throughout an electric interconnection based on changes in phasor angles observed at a limited number of buses.

This work was supported in part by the U.S. National Science Foundation (NSF) awards 0540237 and 0524695, the Power Systems Engineering Research Center, and an NSF Graduate Research Fellowship. Data was also provided by the Tennessee Valley Authority for evaluation of our algorithm.

J. E. Tate and T. J. Overbye are with the Department of Electrical Engineering, University of Illinois at Urbana-Champaign, Urbana, IL 61801 USA (email: jetate1@uiuc.edu, overbye@uiuc.edu)

II. Problem Formulation

The problem addressed is the detection of system events using only PMU data, transmission line and transformer parameter data, and system topology information. One key assumption made is that the fast system dynamics are well-damped and that the system settles down into a quasi-stable state following a system disturbance. Furthermore, although the power flow solutions to the system before and after the event do not take into account system dynamics, it is assumed that the power flow solution after the event will closely match the system values measured after the fast system dynamics have damped out [16].

After the system transients damp out in response to the event, the phasor angle differences at the observable buses in the system with respect to their pre-event values must be determined. Once the changes in angles at each bus has been determined (denoted as the K-dimensional vector $\boldsymbol{\Delta\theta}_{observed}$, where K is the number of phasor angles observable using PMUs), the following optimization problem is solved:

$$E^* = \arg\min_{E \in \mathcal{E}} \left\| \boldsymbol{\Delta\theta}_{observed} - f(E) \right\| \tag{1}$$

where $\mathcal{E}$ is the set of events to be checked for occurrence, and $f(E)$ is a function which relates an event E to the changes in angles caused by the event. Fig. 1 provides a visual depiction of (1), although (1) is K-dimensional while the figure is only 2-dimensional. In this figure, the changes in angles due to the non-minimizing events, $f(E_{1-5})$ are colored gray and the angle change vector from the best matching event, $f(E^*)$, is shown in black.

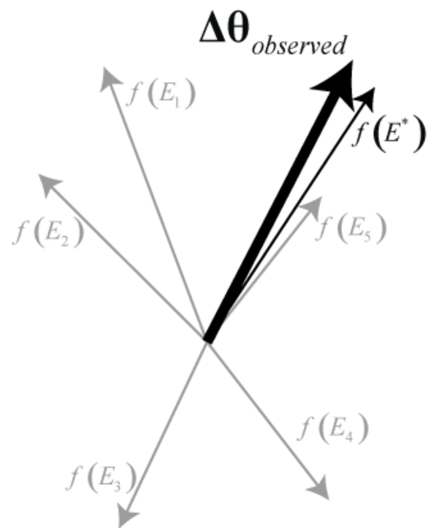

Fig. 1. Determining the event which best matches the observed angle changes

III. Detecting Event Occurrence and Extracting Angle Changes

In order to evaluate the possibility of an event having occurred on the system, it is first necessary to determine the quasi-steady state changes in measured phasor angles, $\mathbf{\Delta\theta}_{observed}$. The phasor angle measurements at bus *i* is referred to as $\theta_i[n]$, where *n* is the *n*th sample of the phasor angle. Because only the quasi-steady state angle values are of interest, rather than the total dynamic response, any fast oscillations in the phasor angles must be filtered out, along with any other noise present in the measurement signals. Therefore, the original angle measurements are filtered with a low-pass filter having a cutoff frequency of 0.2 Hz; the output of this filter is named $\theta_{i,LPF}[n]$ for the phasor angle measurements at bus *i*. An example measurement, along with the low-pass filtered form of the measurement, is given in Fig. 2. This is the same filter method used to show PMU data in [17]. As shown in Fig. 2, the filter eliminates much of the noise in the signal and also the 0.5-3 Hz oscillations typically seen after a line outage. Once the phasor angles have been low-pass filtered, a "candidate" signal $\Delta\theta_{i,candidate}[n]$ is constructed for each bus *i*:

$$\Delta\theta_{i,candidate}[n] = \theta_{i,LPF}[n] - \theta_{i,LPF}[n - N_{trans}] \quad (2)$$

where N_{trans} is a parameter chosen so that the transition portion of the angle change due to the outage (see Fig. 2) is skipped; for the examples presented in this paper, where the sampling frequency is 30 samples per second, N_{trans} is set at 40 samples.

In order to detect whether an event has occurred, a method commonly used in edge detection [18] was adapted for our purposes. Initially, the candidate signal $|\Delta\theta_{i,candidate}[n]|$ is compared against a threshold value τ for the angles measured on the system. After detecting a value of $|\Delta\theta_{i,candidate}[n_{initial}]|$ that is greater than the threshold value for any bus *i*,

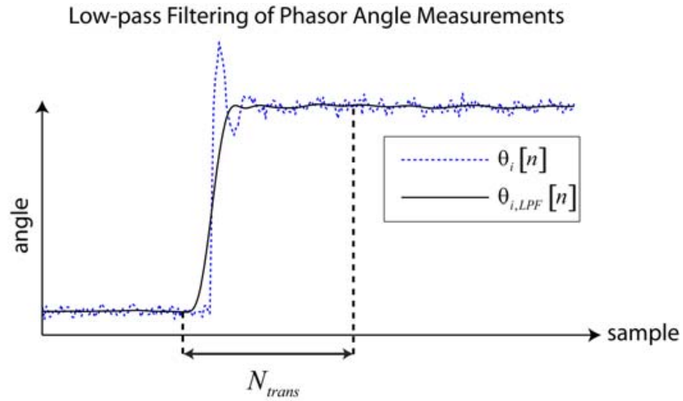

Fig. 2. Low-pass filtering of phasor angle measurements with noise and oscillations

$|\Delta\theta_{i,candidate}[n]|$ is processed for $n > n_{initial}$ until $|\Delta\theta_{i,candidate}[n]|$ begins to decrease. A decrease in $|\Delta\theta_{i,candidate}[n]|$ implies that the maximum of $|\Delta\theta_{i,candidate}[n]|$ has been reached and the $\mathbf{\Delta\theta}_{observed}$ vector is then constructed. The pseudocode for this "hill climbing" procedure, visualized in Fig. 3, is as follows:

$$\begin{aligned}
&\text{if } |\Delta\theta_{i,candidate}[n]| > \tau \text{ at } n = n_{initial} \text{ for any } i,\\
&\quad n_{max} = n_{initial}\\
&\quad \Delta^2\theta_{i,candidate} = \infty\\
&\quad \text{while } (\Delta^2\theta_{i,candidate} \geq \gamma)\\
&\qquad \Delta^2\theta_{i,candidate} = \text{sign}(\Delta\theta_{i,candidate}[n_{max}]) \times\\
&\qquad\quad (\Delta\theta_{i,candidate}[n_{max}+1] - \Delta\theta_{i,candidate}[n_{max}])\\
&\qquad \text{if } (\Delta^2\theta_{i,candidate} > 0) \text{ then}\\
&\qquad\quad n_{max} = n_{max} + 1
\end{aligned} \quad (3)$$

where γ is a parameter which allows very small decreases (for the examples presented below, γ was set to 0.05 degrees) in the midst of continuing increases when determining the maximum value of $|\Delta\theta_{i,candidate}[n]|$ occurs. After n_{max} has been determined according to (3), the observed angle change vector is determined:

$$\mathbf{\Delta\theta}_{observed} = \begin{bmatrix} \Delta\theta_{1,candidate}[n_{max}] \\ \Delta\theta_{2,candidate}[n_{max}] \\ \vdots \\ \Delta\theta_{K,candidate}[n_{max}] \end{bmatrix} \quad (4)$$

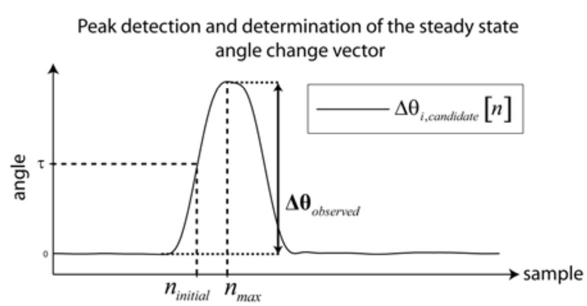

Fig. 3. Peak detection and determination of the observed angle change vector

The threshold value τ must be chosen with care, because setting the threshold value too high might result in missing events that only result in small angle changes, whereas choosing a threshold value which is too low could result in misclassification of noise as an event. Based on analysis of both real and simulated PMU data during line outage events, a threshold of 0.5 degrees was found to be a good compromise.

IV. Single Line Outage Detection Algorithm

A. Analytical basis for line outage detection using quasi-steady state angle changes

If $\mathscr{E}$ is restricted to a set of single line outages on the system, then the problem defined in (1) becomes:

$$\text{line outaged } l^* = \arg\min_{l\in\{1,2,\ldots,L\}}\left(\min_{P_l}\left\|\Delta\boldsymbol{\theta}_{observed} - deltaAngles_l\left(P_l\right)\right\|\right) \tag{5}$$

where L is the number of lines in service before the event is detected and $deltaAngles_l\left(P_l\right)$ is the calculated change in angles that would occur for a pre-outage flow of P_l on line l. Because P_l is allowed to vary in order to achieve the best match in observed and calculated angles, a unique solution of (5) requires that each line outage be distinguishable from the outage of other lines regardless of the pre-outage flow on each line.

Solution of (5) requires the ability to relate the pre-outage flow on a line l to the observed angle changes on that line if it were to be outaged (represented by $deltaAngles_l\left(P_l\right)$). A simple expression for $deltaAngles_l\left(P_l\right)$ is obtained if the dc power flow equations are used. Consider the relationship between changes in power injections and angles based on the dc power flow assumptions:

$$\Delta\boldsymbol{\theta} = \mathbf{B}^{-1}\Delta\mathbf{P} \tag{6}$$

where $\Delta\boldsymbol{\theta}$ is the changes in angles at all system buses due to a change in power injections of $\Delta\mathbf{P}$. The $\mathbf{B}$ matrix used here can be determined using line status information a source of system-wide topology data such as the NERC SDX.

When the dc power flow equations are used, the effect of the outage of a line l can be approximated by a power transfer $\tilde{P}_l$ between the line's "to" bus l_{to} and it's "from" bus l_{from} [19]. The transfer amount can be determined from the following equation:

$$\tilde{P}_l = \frac{P_l}{1 + PTDF_{l,l_{from}-l_{to}}} \tag{7}$$

where P_l is the pre-outage flow on line l defined as positive if flowing from l_{from} to l_{to} and $PTDF_{l,l_{from}-l_{to}}$ is the power transfer distribution factor (PTDF) relating the change in flow on line l due to a transfer from l_{from} to l_{to} [19]. If the power injection $\tilde{P}_l$ is imposed on the system, then a change in angles occurs at all buses. To distinguish the observable angles from the complete set of angles at all buses, a K by N matrix $\mathbf{K}$ is introduced:

$$\mathbf{K} = \begin{bmatrix}\mathbf{I}_{K\times K} & \mathbf{0}_{K\times(N-K)}\end{bmatrix} \tag{8}$$

where K is the number of phasor angles observable from the PMUs, N is the total number of system buses, $\mathbf{I}_{K\times K}$ is the K x K identity matrix, and $\mathbf{0}_{K\times(N-K)}$ is a $K\times\left(N-K\right)$ matrix of zeros. The set of angle changes at the observable buses, which is denoted as $\Delta\boldsymbol{\theta}^{\tilde{P}_l}_{calc,l}$, is then found by applying equation (6):

$$\begin{aligned}\Delta\boldsymbol{\theta}^{\tilde{P}_l}_{calc,l} &= \mathbf{K}\mathbf{B}^{-1}\begin{bmatrix}0\\ \tilde{P}_l\\ -\tilde{P}_l\\ 0\end{bmatrix}\begin{matrix}\\ \leftarrow l_{to}\\ \leftarrow l_{from}\\ \\ \end{matrix}\\ &= \tilde{P}_l\mathbf{K}\mathbf{B}^{-1}\begin{bmatrix}0\\ 1\\ -1\\ 0\end{bmatrix}\begin{matrix}\\ \leftarrow l_{to}\\ \leftarrow l_{from}\\ \\ \end{matrix}\\ &= \tilde{P}_l\Delta\tilde{\boldsymbol{\theta}}_{calc,l}\end{aligned} \tag{9}$$

As shown in (9), the changes in angles are linear with respect to $\tilde{P}_l$; therefore, the calculated changes in angles for a particular pre-outage flow on line l can be written as a scalar $\tilde{P}_l$ multiplying a constant vector $\Delta\tilde{\boldsymbol{\theta}}_{calc,l}$. In turn, (5) can be rewritten with $deltaAngles_l\left(P_l\right)$ replaced by the appropriate scalar-vector product:

$$\text{line outaged } l^* = \arg\min_{l\in\{1,2,\ldots,L\}}\left(\min_{\tilde{P}_l}\left\|\Delta\boldsymbol{\theta}_{observed} - \tilde{P}_l\Delta\tilde{\boldsymbol{\theta}}_{calc,l}\right\|\right) \tag{10}$$

The optimization given in (10) can be performed very quickly using dot products. To see why this is the case, consider two vectors **a** and **b**. From linear algebra, it is known that the projection of **b** onto **a**, $proj_{\mathbf{a}}\mathbf{b}$, is the vector that minimizes **b** - k**a**, where k is allowed to take on any value [20]. The formula for calculating $proj_{\mathbf{a}}\mathbf{b}$ is:

$$\begin{aligned}k^* &= \frac{\mathbf{a}\cdot\mathbf{b}}{\mathbf{a}\cdot\mathbf{a}} = \arg\min_k\left\|\mathbf{b} - k\mathbf{a}\right\|\\ proj_{\mathbf{a}}\mathbf{b} &= k^*\mathbf{a}\end{aligned} \tag{11}$$

Comparing equations (10) and (11), the inner minimization of (10) can be rewritten as:

$$\begin{aligned}\tilde{P}_l^* &= \frac{\Delta\boldsymbol{\theta}_{observed}\cdot\Delta\tilde{\boldsymbol{\theta}}_{calc,l}}{\Delta\tilde{\boldsymbol{\theta}}_{calc,l}\cdot\Delta\tilde{\boldsymbol{\theta}}_{calc,l}}\\ \min_{\tilde{P}_l}\left\|\Delta\boldsymbol{\theta}_{observed} - \tilde{P}_l\Delta\tilde{\boldsymbol{\theta}}_{calc,l}\right\| &= \left\|\Delta\boldsymbol{\theta}_{observed} - \tilde{P}_l^*\Delta\tilde{\boldsymbol{\theta}}_{calc,l}\right\|\end{aligned} \tag{12}$$

The inner minimization can then be eliminated and the complete minimization rewritten using dot products:

$$\text{line outaged } l^* = \arg\min_{l\in\{1,2,\ldots,L\}}\left(\left\|\Delta\boldsymbol{\theta}_{observed} - \left(\frac{\Delta\boldsymbol{\theta}_{observed}\cdot\Delta\tilde{\boldsymbol{\theta}}_{calc,l}}{\Delta\tilde{\boldsymbol{\theta}}_{calc,l}\cdot\Delta\tilde{\boldsymbol{\theta}}_{calc,l}}\right)\Delta\tilde{\boldsymbol{\theta}}_{calc,l}\right\|\right) \tag{13}$$

Because $\Delta\boldsymbol{\theta}_{observed}$ is a fixed vector and $\Delta\tilde{\boldsymbol{\theta}}_{calc,l}$ is scaled by the optimal value to minimize the differences in observed and calculated angle changes, the closeness of fit between the changes in angles due to the outage of line *l* and the observed angle changes is due to the direction associated with each vector. To quantify this relationship, a normalized angle distance metric for a given line *l*, NAD_l, is defined as follows:

$$NAD_l = \min\left\{ \left\| \frac{\Delta\boldsymbol{\theta}_{observed}}{\left\|\Delta\boldsymbol{\theta}_{observed}\right\|} - \frac{\Delta\tilde{\boldsymbol{\theta}}_{calc,l}}{\left\|\Delta\tilde{\boldsymbol{\theta}}_{calc,l}\right\|} \right\|, \left\| \frac{\Delta\boldsymbol{\theta}_{observed}}{\left\|\Delta\boldsymbol{\theta}_{observed}\right\|} + \frac{\Delta\tilde{\boldsymbol{\theta}}_{calc,l}}{\left\|\Delta\tilde{\boldsymbol{\theta}}_{calc,l}\right\|} \right\| \right\} \quad (14)$$

Fig. 4 shows the *NAD* metric and how it relates to the normalized observed and calculated angle changes. As shown in the figure, the closer the direction of the observed and expected angle change vectors, the closer the *NAD* value should be to zero. The minimization in the definition is needed to account for fact that $\tilde{P}_l^*$ can be either positive or negative.

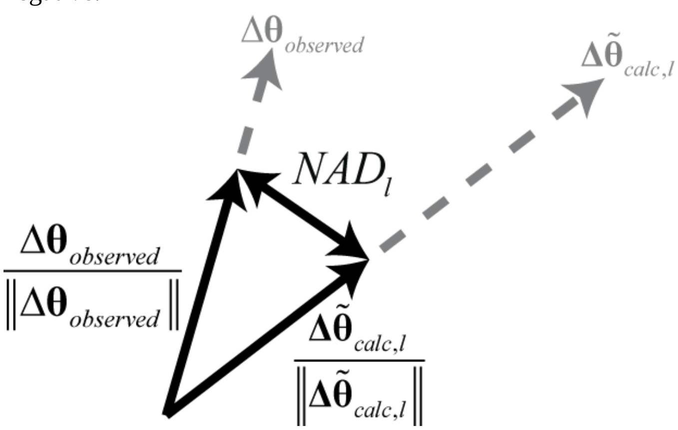

Fig. 4. Normalized angle difference (NAD) metric

B. Basic algorithm definition

In order to detect a line outage, identify the outaged line, and determine the pre-outage flow on that line, the following basic algorithm can be used:

1. Determine whether an outage has occurred by filtering the phasor angles and checking for a change in angles greater than or equal to τ. When a qualifying change is detected, proceed to step 2.
2. Determine the observed angle change vector $\Delta\boldsymbol{\theta}_{observed}$ using (3) and (4).
3. For each line *l*:
   a. Calculate $\Delta\tilde{\boldsymbol{\theta}}_{calc,l}$ using (9).
   b. Calculate $\tilde{P}_l^*$ using (12).
   c. Calculate the error between the measured and expected angle changes for the outage of line *l* using (12) and the results from steps 3a and 3b, then store the calculated error value in the indexed array *AngleError*:

$$AngleError_l = \left\| \Delta\boldsymbol{\theta}_{observed} - \tilde{P}_l^* \Delta\tilde{\boldsymbol{\theta}}_{calc,l} \right\| \quad (15)$$

4. Determine the line l^* that was outaged by sorting *AngleError*:

$$l^* = \arg\min_l AngleError_l \quad (16)$$

5. Determine the pre-outage flow on the line which best fits the observed angle, $P_{l^*}^*$, using (7) and the results from step 3b:

$$P_{l^*}^* = \tilde{P}_{l^*}^* \left(1 + PTDF_{l^*, l^*_{from} - l^*_{to}}\right) \quad (17)$$

C. Computational complexity

To calculate the angle change due to the outage of a line *l* using (9), the **B** matrix must be factored using LU decomposition [21]. This is the most expensive operation in the algorithm, but it only needs to be performed once per change in topology. Once **B** is factored, $\Delta\tilde{\boldsymbol{\theta}}_{calc,l}$ can be quickly computed using forward and backward substitution. Outside of step 3a, the algorithm requires only addition and dot products with vectors of dimension *K* and a sort operation.

D. Algorithm issues

The algorithm as defined in the above section is subject to several possible errors. First, the conditions under which the dc power flow equations hold (low impedance lines, small angle differences across lines, and near-nominal voltages) are necessary in order to treat the power system as a linear system. Because in a real system these conditions are never completely satisfied, error is introduced into the calculation of $\Delta\tilde{\boldsymbol{\theta}}_{calc,l}$ and $\tilde{P}_l^*$ [22]. As a result, the calculated error values from (15) may not accurately reflect the true relationship between the outage of line *l* and the observed angle changes, which could lead to inaccurate line rankings.

Another possible error source is in the determination of $\Delta\boldsymbol{\theta}_{observed}$. Ideally, $\Delta\boldsymbol{\theta}_{observed}$ would correspond precisely to the quasi-steady state angle changes due to the line outage. However, errors in $\Delta\boldsymbol{\theta}_{observed}$ can be caused by inaccurate instrument transformers, analog-to-digital conversion, and the determination of $\Delta\boldsymbol{\theta}_{observed}$ based on (3) and (4).

Still another possible problem arises when multiple lines cause similar changes in phasor angles at the observed buses. Because optimal scaling is performed on the $\Delta\tilde{\boldsymbol{\theta}}_{calc,l}$ vectors, any lines *a* and *b* such that the normalized dot product is close to 1, i.e.,

$$\left| \frac{\Delta\tilde{\boldsymbol{\theta}}_{calc,a}}{\left\|\Delta\tilde{\boldsymbol{\theta}}_{calc,a}\right\|} \cdot \frac{\Delta\tilde{\boldsymbol{\theta}}_{calc,b}}{\left\|\Delta\tilde{\boldsymbol{\theta}}_{calc,b}\right\|} \right| \approx 1 \quad (18)$$

are hard to distinguish with regard to the algorithm. One obvious example where (18) would be true is if the lines *a* and *b* are parallel lines in the system. Although the case of parallel lines being indistinguishable is unavoidable, if (18) holds for non-parallel lines, then PMUs must be added to the system in order to ensure that line outages are distinguishable.

E. Algorithm with heuristics and extended reporting

Considering these complicating factors, modifications were made to the algorithm to aid in correct detection of the outaged line. The first modification is based on the observation that a line which requires a pre-outage flow exceeding the known line limit is most likely not the outaged line. For example, if the pre-outage flow on a line would have to be 100 GW in order to get the observed angle changes and the line's rating is 500 MW, that line is probably not the outaged line. Therefore, lines with pre-outage flows above a cutoff value are removed from consideration after step 3. For the examples given below, the cutoff was set to twice the line rating or 5 GW if a line limit was not known, although for a real system it is likely that these limits would be known for all lines of interest.

In addition to this refinement, the pre-outage flows calculated using (17) are presented along with line rankings. This allows the user to apply engineering judgment in deciding if pre-outage flows are reasonable. This modification requires that step 4, which initially provided only the most likely line to be outaged, be replaced by a set of steps which returns the *X* most likely lines to be outaged:

4'. For *rank* = 1 to *X*

a. $LineRanked_{rank} = l^*_{rank} = \arg\min_{l} AngleError_l$

b. $AngleError_{l^*_{rank}} = +\infty$

With this modification, the line returned in step 4 of the original algorithm is $LineRanked_1$. To construct the tables of results given below in the examples, *X* was set to five. Additional knowledge, such as known direction of flow, could also be easily incorporated into the algorithm.

V. EXAMPLES

In order to gauge the effectiveness of our algorithm, the algorithm was tested on two systems—a 37 bus study system and the Tennessee Valley Authority (TVA) control area—with simulated and real data, respectively.

A. 37 bus study system simulated outage

To ascertain the ability of the algorithm to correctly detect and identify line outages, the algorithm was tested using a 37 bus, 9 generator system with an average R/X ratio of 0.378 taken from Example 13.9 in [24]. The generators were modeled as round rotor machines with quadratic saturation using an IEEE Type 1 exciter. A oneline diagram of the system is provided in Fig. 5. To examine the performance of the algorithm, dynamic simulations were run using PowerWorld Simulator to simulate the PMU data that would be obtained after the outage of the SAVOY138-JO138 line, indicated in Fig. 6. Before the outage, the power flow on the line is 73 MW from JO138 to SAVOY138.

The system was simulated with PMUs located at buses TIM138, SLACK345, and LAUF69 (see Fig. 6). The simulated phasor angles at the TIM138 and LAUF69 buses, with SLACK345 used as the reference bus, are shown in Fig. 7.

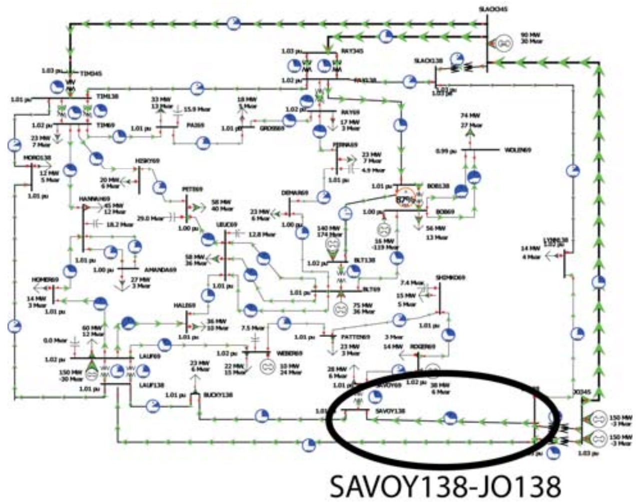

Fig. 5. Oneline diagram of 37 bus study system

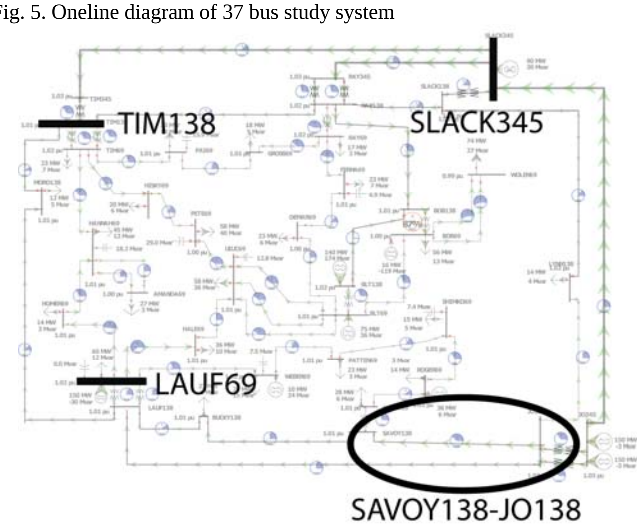

Fig. 6. PMU configuration and outage location for 37 bus test system

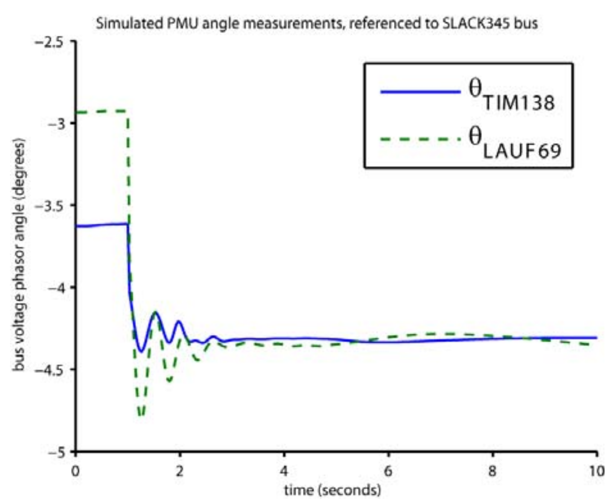

Fig. 7. Simulated angle measurements for the 37-bus system outage

Table I shows the results of running the algorithm with these bus angle measurements. The correct line is detected, and the calculated pre-outage flow on the line is only 5% away from the correct pre-outage flow value. Also, the *NAD* value for the correct line is 0.003, whereas the line ranked second has a much greater *NAD* value (0.023). Therefore, with only three PMUs on a 37 bus system, the algorithm accurately detects the line outage.

TABLE I
37 BUS SYSTEM RESULTS USING SIMULATED MEASUREMENTS

Rank	Line	Pre-outage flow (MW)	*NAD*
1	JO138-SAVOY138	69	0.003
2	RAY138-BOB138	90	0.023
3	BOB138-BLT138	247	0.023
4	BLT138-BLT69	247	0.023
5	JO138-LAUF138	80	0.036

The angle values used in determining Table I were taken directly from the dynamic simulation without any noise added to the signal. To see the effects of noise on the algorithm, zero mean Gaussian noise with a standard deviation of 0.1 degrees was added to the simulated phasor angles. The angle measurements obtained are shown in Fig. 8, and the results of running the algorithm with these measurements are given in Table II. The difference between the calculated pre-outage flow value and the correct value is 3% for the results based on the noisy measurements, which is an improvement over the noiseless measurement result. One possible explanation for this is that the addition of Gaussian noise cancels out some of the oscillations. The *NAD* value, however, has gone up significantly, from 0.003 to 0.013. This is still a low value, but it does show that the presence of noise in the angle measurements can have a negative impact on the estimation of the steady state angle differences and result in a higher *NAD* value.

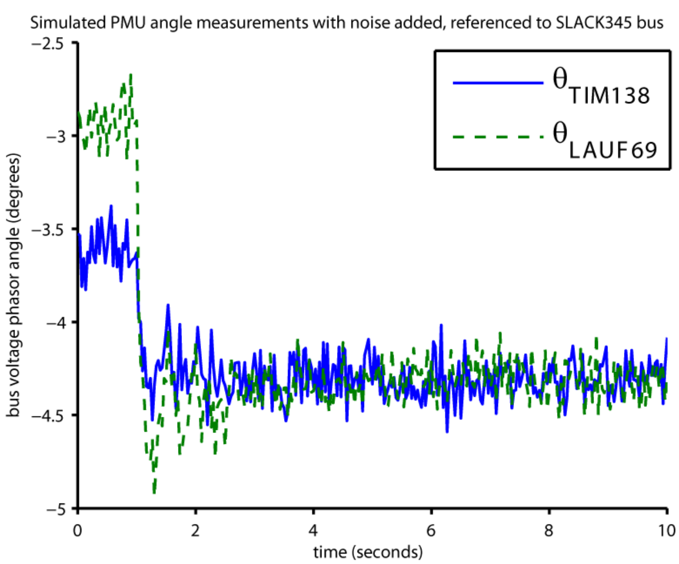

Fig. 8. Simulated angle measurements for the 37-bus system with noise added

TABLE II
37 BUS SYSTEM RESULTS WITH GAUSSIAN NOISE ADDED TO MEASUREMENTS

Rank	Line	Pre-outage flow (MW)	*NAD*
1	JO138-SAVOY138	71	0.013
2	RAY138-BOB138	92	0.033
3	BOB138-BLT138	253	0.033
4	BLT138-BLT69	253	0.033
5	JO138-LAUF138	82	0.046

B. TVA 500 kV line outage with real PMU data

The following example details the performance of the algorithm using real PMU data during a line outage in the TVA control area, with a system model consisting of 7013 buses. Real data is being shown in this example; however, due to data confidentiality issues, detailed bus and line information is not provided.

State estimator case files were used to construct the **B** matrix. The event analyzed in this example is the outage of a 500 kV line carrying (according to a state estimator case) 1072 MW. On the system, there were seven PMUs deployed, each providing data at 30 samples per second. One of the buses for which PMU data was available was chosen as the reference bus. The angle measurements from the other buses were then subtracted from the reference bus angles.

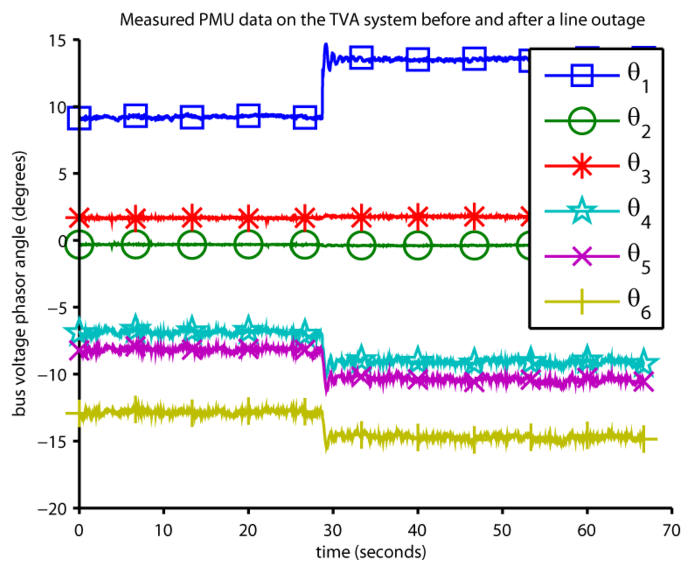

Fig. 9. Line outage PMU measurements on the TVA system before and after the line outage

Fig. 9 shows the referenced PMU angle measurements before and after the line outage. Clearly, there is a significant steady state angle change in several of the PMU measurements, particularly for θ_1, θ_4, θ_5, and θ_6. Also, note that there are oscillations and noise in all of the angle measurements. However, once the low-pass filter described in the above section is applied, much of the noise and oscillations are removed. As an example, Fig. 10 shows how low-pass filtering attenuates both the noise and low frequency oscillations in the angle measurements θ_1.

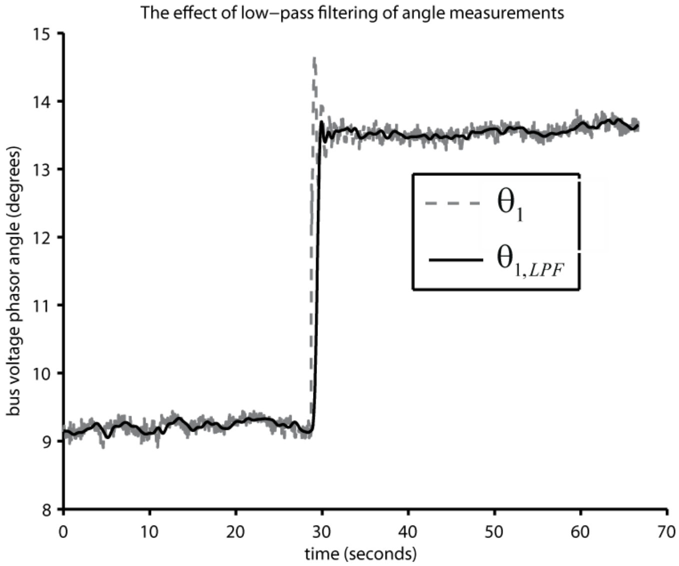

Fig. 10. Effect of low-pass filtering on real phasor angle measurements

Using the procedure given in (3), $\mathbf{\Delta\theta}_{observed}$ was calculated and the following values were obtained:

$$\mathbf{\Delta\theta}_{observed} = \begin{bmatrix} \Delta\theta_1 \\ \Delta\theta_2 \\ \Delta\theta_3 \\ \Delta\theta_4 \\ \Delta\theta_5 \\ \Delta\theta_6 \end{bmatrix} = \begin{bmatrix} 4.55^\circ \\ -0.06^\circ \\ 0.12^\circ \\ -2.24^\circ \\ -2.11^\circ \\ -1.90^\circ \end{bmatrix} \quad (19)$$

After $\mathbf{\Delta\theta}_{observed}$ was determined, the algorithm was run to predict the outaged line along with the pre-outage flow. The results from the algorithm are shown in Table III. The algorithm correctly determines the outaged line, referred to by the identifier 1466. Also, the pre-outage flow calculated by the algorithm, 1058 MW, is only 1% different from the state estimator value of 1072 MW. Another key feature of the results shown is that the *NAD* value for the correct line, 0.015, is significantly lower than the 0.311 *NAD* value for the line ranked second.

TABLE III
ALGORITHM RESULTS FOR TVA SYSTEM LINE OUTAGE

Rank	Line ID	Pre-outage flow (MW)	*NAD*
1	1466	1058	0.015
2	4801	2722	0.311
3	1708	1087	0.524
4	3118	4870	0.570
5	1625	891	0.630

Because one of the angle measurements, θ_1, is taken from a terminal bus of the outaged line, it is also interesting to see how the algorithm performs when this angle measurement is removed. With this angle removed, $\mathbf{\Delta\theta}_{observed}$ was determined to be:

$$\mathbf{\Delta\theta}_{observed} = \begin{bmatrix} \Delta\theta_2 \\ \Delta\theta_3 \\ \Delta\theta_4 \\ \Delta\theta_5 \\ \Delta\theta_6 \end{bmatrix} = \begin{bmatrix} -0.06^\circ \\ 0.13^\circ \\ -2.29^\circ \\ -2.21^\circ \\ -1.99^\circ \end{bmatrix} \quad (20)$$

As shown in Table IV, the algorithm still correctly detects the outaged line and determines the pre-outage flow with only a 1% difference from the state estimator flow value on the line. The main difference between the results in Table III and Table IV is that the differentiation between the *NAD* values of the correct line and the line ranked second is much smaller in Table IV. This indicates that increasing the PMU information available allows for better differentiation between outaged lines. One other point of interest is that the line with identifier 1685 shares a bus with the correctly outaged line; therefore, if these results were visualized on a one-line display, the method presented here would still be a useful indicator of where the outage occurred in the system even if the rankings were switched.

TABLE IV
ALGORITHM RESULTS FOR TVA SYSTEM LINE OUTAGE WITH TERMINAL ANGLE MEASUREMENT θ_1 REMOVED

Rank	Line ID	Pre-outage flow (MW)	*NAD*
1	1466	1082	0.013
2	1685	750	0.033
3	2622	4703	0.038
4	2614	4769	0.038
5	1684	1084	0.066

VI. CONCLUSIONS AND FUTURE WORK

The satisfactory performance of the algorithm with both real data and simulated data on large and small power systems indicates that it is possible to use PMU data, even when coverage is extremely limited, to detect system events. The results also indicate that knowledge of topology changes outside of the local control area could be obtained by using data which is currently available on the North American power grid. In addition, the presence of measurement noise and oscillatory behavior does not have a catastrophic effect on the algorithm's performance. Therefore, this algorithm can currently provide a robust way to increase operator awareness of line statuses throughout an electric interconnection.

One of our goals in future research is to expand the event types detected to include sequential and simultaneous multiple line outages along with generator outages. We are also interested in exploring the usage of phasor magnitude and frequency data, as these data values are unused in the current event detection algorithm. Finally, because the research thus far has shown that incomplete PMU coverage can be used in event detection, we are investigating ways that limited PMU placement can be optimized in order to detect events of interest.

VII. References

[1] US-Canada Power System Outage Task Force, Final Report on the August 14, 2003 Blackout in the United States and Canada, pp. 104-107, Apr. 2004. [Online]. Available: https://reports.energy.gov/BlackoutFinal-Web.pdf.

[2] "Steps to Establish a Real-Time Transmission Monitoring System for Transmission Owners and Operators Within the Eastern and Western Interconnections," U.S. Department of Energy and Federal Energy Regulatory Commission, Feb. 2006.

[3] A. G. Phadke, "Synchronized phasor measurements in power systems," *IEEE Comput. Appl. Power*, vol. 6, no. 2, pp. 10-15, Apr. 1993.

[4] M. Donnelly, M. Ingram, and J. R. Carroll, "Eastern Interconnection Phasor Project," *Proc. 39th Hawaii Int'l Conf. System Sciences*, pp. 336-342, Jan. 2006.

[5] W. Jiang, V. Vittal, and G. T. Heydt, "A distributed state estimator utilizing synchronized phasor measurements," *IEEE Trans. Power Syst.*, vol. 22, no. 2, pp.563-571, May 2007.

[6] M. Zhou, V. A. Centeno, J. S. Thorp, and A. G. Phadke, "An alternative for including phasor measurements in state estimators," *IEEE Trans. Power Syst.*, vol. 21, no. 4, pp. 1930-1937, Nov. 2006.

[7] J. S. Thorp, A. G. Phadke, and K. J. Karimi, "Real time voltage-phasor measurements for static state estimation," *IEEE Trans. Power App. Syst.*, vol. PAS-104, no. 11, pp. 3098-3106, Nov. 1985.

[8] A. P. S. Meliopoulos, G. J. Cokkinides, O. Wasynczuk, E. Coyle, C. Hoffmann, C. Nita-Rotaru, T. Downar, L. Tsoukalas, and R. Gao, "PMU Data Characterization and Application to Stability Monitoring," *2006 IEEE Power Engineering Society Power Syst. Conf. and Expo.*, pp. 151-158, Nov. 2006.

[9] K. Sun, S. Likhate, V. Vittal, V. S. Kolluri, and S. Mandal, "An online dynamic security assessment scheme using phasor measurements and decision trees," *IEEE Trans. Power Syst.*, vol. 22, no. 4, pp. 1935-1943, Nov. 2007.

[10] A. R. Khatib, R. F. Nuqui, M. R. Ingram, and A. G. Phadke, "Real-time estimation of security from voltage collapse using synchronized phasor measurements," *Proc. IEEE Power Eng. Soc. General Meeting, 2004*, vol. 1, pp. 582-588, Jun. 2004.

[11] G. Zhang, P. Hirsch, and S. Lee, "Wide area frequency visualization using smart client technology," *Proc. IEEE Power Eng. Soc. General Meeting, 2007*, pp. 1-8, Jun. 2007.

[12] R. Klump, R. E. Wilson, and K. E. Martin, "Visualizing real-time security threats using hybrid SCADA / PMU measurement displays," in *Proc. 38th Hawaii Int'l Conf. Syst. Sciences*, Jan. 2005.

[13] S. Chun-Lien and J. Bo-Yuan, "Visualization of large-scale power system operations using phasor measurements," in *Proc. Int'l Conf. Power Syst. Tech., 2006*, Oct. 2006.

[14] US-Canada Power System Outage Task Force, Final Report on the August 14, 2003 Blackout in the United States and Canada, p. 51, Apr. 2004. [Online]. Available: https://reports.energy.gov/BlackoutFinal-Web.pdf.

[15] US-Canada Power System Outage Task Force, Final Report on the Implementation of the Task Force Recommendations, pp. 36-38, Sep. 2006. [Online]. Available: http://www.oe.energy.gov/DocumentsandMedia/BlackoutFinalImplementationReport(2).pdf.

[16] R. Yeu and P. Sauer, "Post-contingency equilibrium analysis techniques for power systems", *Proc. 37th North American Power Symp.*, pp. 429-433, Oct. 2005.

[17] J. Hauer, N. Bhatt, K. Shah, and S. Kolluri, "Performance of 'WAMS East' in Providing Dynamic Information for the North East Blackout of August 14, 2003", *Proc. IEEE Power Eng. Soc. General Meeting, 2004*, pp. 1685-1690, Jun. 2004.

[18] D. Forsyth and J. Ponce, *Computer Vision: A Modern Approach*, New Jersey: Prentice Hall, 2003, pp. 176-179.

[19] P. Sauer, K. Reinhard, and T. Overbye, "Extended factors for linear contingency analysis", *Proc. 34th Hawaii Int'l Conf. System Sciences*, pp. 697-703, Jan. 2001.

[20] H. Anton, *Elementary Linear Algebra, 8th Edition*, New York: Wiley, 2000, pp. 303-312.

[21] M. Crow, *Computational Methods for Electric Power Systems*, Boca Raton: CRC Press, 2003.

[22] R. Kaye and F. Wu, "Analysis of linearized decoupled power flow approximations for steady-state security assessment," *IEEE Trans. Circuits Syst.*, vol. 31, no. 7, pp. 623-636, Jul. 1984.

[23] *IEEE Standard Requirements for Instrument Transformers*, IEEE Standard C57.13-1993, Jul. 1993.

[24] J. Glover, M. Sarma, and T. Overbye, *Power System Analysis and Design, 4th Edition*, United States: Thomson Engineering, 2008.

VIII. Biographies

Joseph Euzebe Tate (S'03) received the B.S. degree in electrical engineering from Louisiana Tech University, Ruston, LA, in 2003 and the M.S. degree in electrical and computer engineering from the University of Illinois at Urbana-Champaign in 2005. Currently, he is working toward the Ph.D. degree in the Department of Electrical and Computer Engineering at the University of Illinois at Urbana-Champaign.

Thomas J. Overbye (S'87-M'93-SM'96-F'06) received the B.S., M.S. and Ph.D. degrees in electrical engineering from the University of Wisconsin-Madison. He is currently the Fox Family Professor of Electrical and Computer Engineering at the University of Illinois at Urbana-Champaign. He was with Madison Gas and Electric Company, Madison, WI, from 1983-1991. His current research interests include power system visualization, power system analysis, and computer applications in power systems.